DEA Dynamics of Chlorine Dioxide Probed by Velocity Slice Imaging

Krishnendu Gope,[a#] Nigel Mason[b], E. Krishnakumar_[a‡] and Vaibhav S. Prabhudesai[a*]

[a]Tata Institute of Fundamental Research, Homi Bhabha Road, Colaba, 400005 Mumbai, India

[b]School of Physical Sciences, University of Kent, Canterbury, CT2 7NH, UK

* Email: vaibhav@tifr.res.in

Present address: Institute of Chemistry, The Hebrew University of Jerusalem, 9190401, Israel

‡ Present address: Raman Research Institute, Sadashiva Nagar, 560080 Bengaluru, India

Abstract:

We report for the first time, detailed dynamics of dissociative electron attachment to the atmospherically important chlorine dioxide (OClO) molecule exploring all the product anion channels. Below 2 eV, the production of vibrationally excited OCl^- dominates the DEA process whereas at electron energies greater than 2 eV, three-body dissociation is found to result in O^- and Cl^- production. We find that the internal energy of OCl^- and the kinetic energy of Cl^- are large enough for them to be relevant in the ozone-depleting catalytic cycle and more investigations on the reaction of these anions with ozone are necessary to completely understand the role of DEA to OClO in ozone depletion. These results also point to an urgent need for comprehensive theoretical calculations of the DEA process to this atmospherically important molecule.

1. Introduction

Chlorine dioxide (OClO) has attracted considerable interest as an atmospherically important molecule due to its role in ozone (O_3) chemistry of the stratosphere. Photodissociation of OClO produces chlorine monoxide radical (OCl) which plays a critical role in the depletion of stratospheric ozone[1, 2] via a catalytic cycle[3-5]. The catalytic cycles involving OCl radical that result in the destruction of ozone are understood to be[2,4-6]

$$\left.\begin{array}{c} OCl + OCl + M \rightarrow (OCl)_2 + M \\ (OCl)_2 + light \rightarrow Cl + ClOO \\ ClOO + M \rightarrow Cl + O_2 + M \\ 2(Cl + O_3 \rightarrow OCl + O_2) \\ Net: 2O_3 \rightarrow 3O_2 \end{array}\right\} \quad (1)$$

$$\left.\begin{array}{c} OCl + BrO \rightarrow Br + ClOO \\ ClOO + M \rightarrow Cl + O_2 + M \\ Br + O_3 \rightarrow BrO + O_2 \\ Cl + O_3 \rightarrow OCl + O_2 \\ Net: 2O_3 \rightarrow 3O_2 \end{array}\right\} \quad (2)$$

$$\left.\begin{array}{c} OCl + HO_2 \rightarrow HOCl + O_2 \\ HOCl + light \rightarrow OH + Cl \\ OH + O_3 \rightarrow HO_2 + O_2 \\ Cl + O_3 \rightarrow OCl + O_2 \\ Net: 2O_3 \rightarrow 3O_2 \end{array}\right\} \quad (3)$$

$$\left.\begin{array}{c} OCl + O_3 \rightarrow ClOO + O_2 \\ ClOO + M \rightarrow Cl + O_2 \\ Cl + O_3 \rightarrow OCl + O_2 \\ Net: 2O_3 \rightarrow 3O_2 \end{array}\right\} \quad (4)$$

In the last direct reaction of OCl radical with ozone, it was found that internal excitation is required to cross the barrier for the reaction in order to have reasonable rates[2]. However, atomic Cl can also cause the ozone destruction, which is more efficient than the other paths[5]. In the stratosphere, OClO acts as a reservoir for OCl radicals especially during arctic winters[2].

In the short wavelength (273 nm to 293 nm) photolysis of OClO, this radical is formed with an internal excitation as high as v=17 vibrational level[7]. There is also minor channel, which results in the production of Cl + O_2 via photoisomerization of OClO to ClOO[8-10]. However, it has been pointed out that the photodissociation cross section to form OCl is as low as 10^{-21}cm^2 and hence may not play a significant role in the ozone destruction cycle[11]. Another route for formation of atomic chlorine (Cl) & OCl from OClO is by dissociative electron attachment (DEA). In this process, in addition to the neutral fragments their anion counterparts Cl^- and OCl^- are also formed. The formation of OCl^- channel is known to be extremely efficient with the measured cross section in the range high 10^{-16} cm^2 [12,13]. Polar stratospheric clouds contain a large number of particles with excess electrons whose binding energy varies from less than 1 eV to several eV. During the Arctic spring, such low energy electrons may be released by UV light and can easily be captured by the OClO leading to the production of OCl^- and Cl atom through DEA[13]. Thus, it is important to investigate the dynamics of the DEA process to OClO in order to understand its implication in ozone chemistry in the upper atmosphere.

DEA to OClO has been studied experimentally by Meinke *et al.*[12], Marston *et al.*[14] and Senn *et al.*[13] but only one theoretical calculation, that by Baluja *et al.*[15] exists. The measurements show the formation of OCl^-, Cl^-, O_2^- and O^-. Three peaks have been reported in the DEA process around 0.7 eV, 4 eV, and 8 eV. The 0.7 eV peak is dominated by OCl^- followed by Cl^- and O_2^- (in order of decreasing intensity). At 4 eV and 8 eV peaks, the Cl^- signal is found to be dominant. Marston *et al.*[10] observed two additional peaks around 0 eV and 6 eV in their measured total negative ion signal from DEA to OClO, however, they have attributed these peaks to the contamination from molecular chlorine present in their sample. Meinke *et al.*[12] and Senn *et al.*[13] have reported a distinct structure in the Cl^- channel around 1.7 eV and identified it with the onset for the three-body break up threshold (Table 1). Senn *et al.*[13] have also observed the O^- signal peaking around 1.15 eV, 4 eV, and 8 eV and a weak structure at 0.28 eV near threshold in OCl^- channel. They determined the total DEA cross section at 0.7 eV peak to be $8x10^{-16}$ cm^2.

Meinke *et al.*[12], Marston *et al.*[14] and Senn *et al.*[13] also measured the kinetic energy (KE) of selected fragments. According to Meinke *et al.*[12], at 0.7 eV incident electron energy the mean KE of Cl^- is about 1 eV, which indicates faster dissociation in the Cl^- channel compared to the O_2^- channel. The measurement of KE of the Cl^- ion using a cylindrical mirror analyzer was carried out by Marston *et al.*[14] for electron energies > 3 eV. They observed that at the 4.3 eV peak, Cl^- ions are produced with thermal KE, whereas at the 8 eV peak the Cl^- KE increases up to 0.5 eV. From energy considerations, they concluded that three-body dissociation might be taking place at 4.3 eV. From the low KE of Cl^- they noted that if the dissociation is due to a concerted three-body break-up, either excited O atoms are produced or the transient $OClO^-$ is nearly linear. Based on the excited state energies of parent neutral OClO, DEA at electron energies below 2 eV has been attributed to a shape resonance. From the bonding nature of the $3b_1$ orbital, this resonance has been assigned to the $^3B_1$ state by Marston *et al.*[14]. The peaks at higher electron energies have then been attributed to core-excited resonances. By analyzing the peaks in the time of flight spectra, Senn *et al.*[13] found the KE of the Cl^- ions to be 0.42 eV and the KE of the O_2^- ions as 0.7 eV at 0.7 eV electron energy. Based on these observations it was concluded that the neutral O_2 is produced with more than 3 eV as its vibrational energy and O_2^- is produced with moderate excitation. Senn *et al.*[13] also noted that the weak structure at 1.7 eV in Cl^- channel coincides with the energy threshold

of three-body dissociation ($Cl^- + O + O$) and the two peaks at 4 eV and 8 eV in both Cl^- and O^- channels are associated with core-excited resonances.

Baluja *et al.*[15] observed several $OClO^-$ anion states in their calculations using the R-matrix method. They reported the $OClO^-$ anion ground state (X^1A_1) to be 1.558 eV below the OClO ground state and found several shape resonances of $^3B_1$, $^1B_1$, $^3A_2$, and $^1A_2$ symmetries at 2.96 eV, 5.75 eV, 7.22 eV and 8.06 eV with widths of 0.843 eV, 1.4 eV, 1.5 eV and 2.72 eV respectively. Wei *et al.*[16] have reported the excited anion states in the energy range of 0 to 3 eV from neutral ground state by performing quantum chemical calculations using a complete active space self-consistent field method with a large atomic natural orbital basis set.

Although KE measurements for Cl^- have been reported for all the peaks and that for O^- and O_2^- has been reported for the 0.7 eV peak, there is no information about the KE of OCl^- or for O^- ions at higher energies. Also, the literature on DEA to OClO is devoid of any measurement of the angular distribution of the fragment ions. Here we report the KE and angular distributions of various fragments arising from DEA to OClO using velocity slice imaging (VSI) technique and from these measurements unravel the underlying dynamics of its excited anion states.

2. Experimental

The experiments were carried out using a VSI set up similar to that originally developed by Nandi *et al.*[17]. The details of the present set up have been described earlier[18-21]. In brief, an effusive molecular beam produced by a capillary interacts with a magnetically collimated pulsed electron beam (200 ns) at right angles. The molecular beam is directed along the axis of the VSI spectrometer. The VSI spectrometer consists of a single element electrostatic lens followed by a flight tube. A 2-D position sensitive detector (PSD) that consists of a set of three 75 mm diameter microchannel plates mounted in a Z-stack configuration followed by a phosphor screen is used to obtain the ion signal. The ions produced in the interaction region are extracted by applying a pulsed electric field with a 100 ns delay with respect to the electron beam pulse. These ions are then velocity focused onto the 2D PSD detector by applying appropriate voltages to the electrodes. The detector is operated in active mode only for 100 ns by applying a 2 kV pulse to the detector with appropriate bias. We record the central slice of the Newton sphere of the ions formed by suitably delaying the 2kV pulse with respect to the extraction pulse. The pixel images formed on the

phosphor screen are recorded by a CCD camera. By applying appropriate calibration, we then convert our pixel images into momentum images and obtain the kinetic energy and angular distribution of the anion fragments. We have used the O^- from DEA to O_2 and Cl^- from DEA to Cl_2 to calibrate the electron energy as well as the VSI spectrometer's momentum scale[17,19].

Due to its highly reactive and explosive nature at ambient temperature and pressure, OClO must be prepared carefully onsite before performing measurements. As its decomposition rate is low on the glass surface, we have prepared the OClO gas in an all glass apparatus which has been further shielded from the UV light to avoid photodissociation using aluminum foil. The preparation of OClO is carried out by oxidation of molecular chlorine using sodium chlorite as prescribed earlier by Derby and Hutchison[22].

$$2NaClO_2 + Cl_2 \rightarrow 2OClO + 2NaCl \quad (5)$$

A mixture of chlorine and He as buffer gas is allowed to flow through a U-tube packed with sodium chlorite. In order to increase the flow rate the salt is mixed with glass beads. The OClO gas (yellow-green) produced via this reaction is then collected along with the He buffer gas in the ratio of 1:4 into a glass container. This mixture is then used for the experiment. The base pressure in the experimental set up is 1 x 10^{-9} Torr. During the experiment the background pressure is maintained at 8x10^{-7} Torr and the maximum target pressure in the effusive beam is estimated to be an order of magnitude higher.

3. Results & Discussion

DEA to OClO leads to the formation of OCl^-, Cl^-, O_2^- and O^- ions. The ion yield curves of each ion recorded in the present experiment are shown in Fig 1. For velocity slice imaging, one needs to stretch the Newton sphere along the time of flight axis. This leads to limited mass resolution in our VSI spectrometer. Due to this, we were unable to resolve Cl^- from O_2^-. As can be seen in Fig 1, the O^- ion yield peaks around 1.1 eV, 4 eV, and 8 eV. The combined signal due to Cl^- and O_2^- channel peaks around 0.7 eV, 4 eV and 8 eV, whereas the OCl^- yield peaks around 0.7 eV. OCl^- is the most dominant channel below 2 eV as can be seen in the relative intensities in Fig. 1. Previous reports[12,13] have shown that both O_2^- and Cl^- are produced below 2 eV whereas at higher energies only Cl^- is present in the 32-35 mass range. Our measurements are consistent with this. However, we cannot clearly discern the weak structure at 1.7 eV in the Cl^- channel as reported earlier. This

is probably due to the poor electron beam resolution (~ 0.6 eV) in the present experiment. We do not see any signal due to molecular chlorine contamination as we compare the measured spectra with those measured for DEA to molecular chlorine (Cl_2) in the same experimental set up[19].

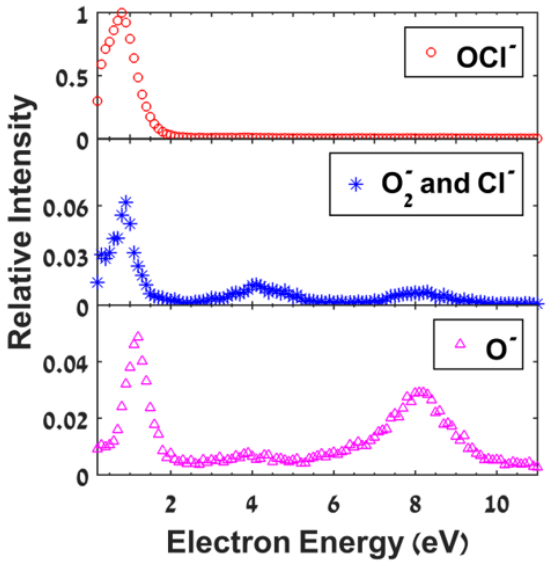

Fig. 1 Yield curves for various anions formed in DEA to OClO.

For ease of interpreting our results, we list all possible DEA channels for the observed fragment ions and their energy thresholds in Table 1.

Table 1 DEA channels in OClO along with threshold energy of the corresponding channel.

	Dissociation Channel	Thermodynamic Threshold (eV)
1	$OClO + e^- \rightarrow OCl^-(X^2\Sigma^+) + O(^3P)$	0.27
2	$OClO + e^- \rightarrow OCl^-(X^2\Sigma^+) + O(^1D)$	2.24
3	$OClO + e^- \rightarrow OCl^-(X^2\Sigma^+) + O(^1S)$	4.46
4	$OClO + e^- \rightarrow Cl^- + O_2(X^3\Sigma_g^-)$	-3.43
5	$OClO + e^- \rightarrow Cl^- + O_2(a^1\Delta_g)$	-2.45
6	$OClO + e^- \rightarrow Cl^- + O_2(b^1\Sigma_g^+)$	-1.79
7	$OClO + e^- \rightarrow Cl^- + O(^3P) + O(^3P)$	1.73
8	$OClO + e^- \rightarrow O_2^- + Cl(^2P)$	-0.27
9	$OClO + e^- \rightarrow O^- + OCl(X^2\Pi)$	1.09
10	$OClO + e^- \rightarrow O^- + OCl(A^2\Pi)$	5.01

11	$OClO + e^- \rightarrow O^- + Cl(^2P) + O(^3P)$	3.88

The thermodynamic thresholds are calculated using ΔH_{0f} (OClO) = 1.08 eV, ΔH_{0f}(OCl) = 1.05 eV[23], ΔH_{0f}(O) = 2.58 eV, ΔH_{0f}(Cl) = 1.26 eV[24]. The relevant electron affinities (EA) are EA (OCl) = 2.28 eV[25], EA (O_2) = 0.45 eV[26], EA (O) = 1.46 eV[27] and EA (Cl) = 3.61 eV[28]. O_2 excitation energies used are 0.98 eV and 1.64 eV for $a^1\Delta_g$ and $b^1\Sigma^+_g$ states respectively[29]. O excitation energies are 1.97 eV and 4.19 eV for ^1D and ^1S states respectively[30]. The OCl electronic excitation energy for $A^2\Pi$ state is taken as 3.92 eV[29]. Below we discuss the results obtained for various ions.

3.1 OCl^- channels

The most dominant channel, namely OCl^-, exhibits only one peak around 0.7 eV that extends up to 1.7 eV. OCl^- can be formed only via asymmetric dissociation of the parent anion. In this type of dissociation, the cleavage of one bond results in rotational motion of the OCl^- due to the bend geometry of the precursor ($OClO^-$). Under the simple impact approximation, where we assume that the dissociation starts at the equilibrium geometry of the parent molecule with an asymmetric stretch mode leading the process and ignoring the role of bending mode, the rotational kinetic energy of the OCl^- fragment is given by[31,32]

$$E_{Rot} = \frac{E_{Excess}}{\left(\frac{f}{cos^2(\beta-90)}+1\right)} \quad (6)$$

where, β is the bond angle of the dissociating $OClO^-$ ion, $f = \frac{2m_O m_{Cl}+m_{Cl}^2}{m_O^2}$ with m_O and m_{Cl} are the mass of O and Cl atoms respectively. E_{Excess} is the excess energy available in the system which is given by

$$E_{Excess} = E_e - E_{Threshold} \quad (7)$$

where $E_{Threshold}$ is the threshold energy for a given channel (here OCl^-) and E_e is the electron energy. Thus, for the equilibrium bond angle of 117.5^0 of OClO[15], about 9% of the excess energy will appear as the rotational energy of OCl^-.

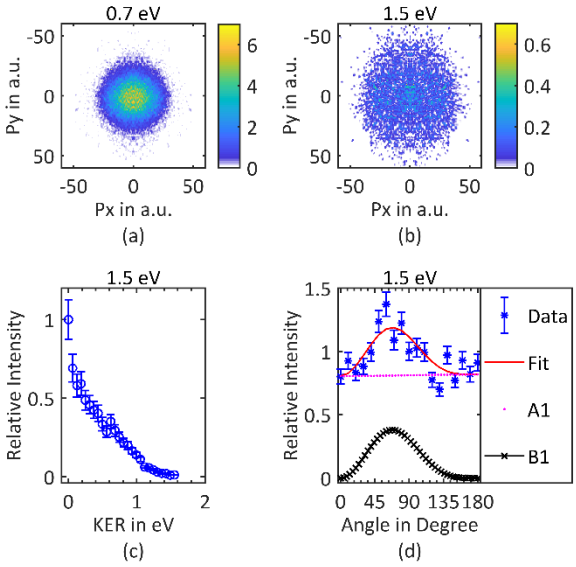

Fig. 2 Momentum images of OCl^- at (a) 0.7 eV and (b) 1.5 eV. The direction of the electron beam is from top to bottom (c) KER obtained from the momentum image of OCl^- at 1.5 eV and (d) the angular distribution of the outer ring of the same image for KER ranging from 0.4 eV to 1.2 eV. A_1 and B_1 are the symmetries of the $OClO^-$ states to which the angular distribution data is fitted.

The momentum images of OCl^- obtained at 0.7 and 1.5 eV are shown in Fig 2. The 0.7 eV image (Fig. 2(a)) shows an isotropic blob corresponding to low KE, extending up to 0.13 eV. The corresponding kinetic energy release (KER) in this channel would be up to 0.55 eV. This is in fair agreement with the expected maximum KER of 0.39 eV based on the threshold of 0.27 eV (Table 1) for the formation of OCl^- + O (^3P) and the rotational energy given by Eq. 6. The slightly larger measured KER may be attributed to the poor electron energy resolution in this experiment as well as to the deviation from the equilibrium geometry of the parent anion at the time of dissociation, which may modify the rotational energy.

At 1.5 eV the KER distribution peaks at 0 eV and extends up to 1.2 eV (Fig 2(c)). As the threshold for the formation of OCl^- with O atom in ^1D state is 2.24 eV (Table 1), only OCl^- + O (^3P) channel contributes to OCl^- signal. The KER distribution shows vibrational excitation of the OCl^- fragment apart from the rotational excitation based on Eq. 6. One may note that the electron detachment threshold of 2.28 eV[25] for OCl^- allows for considerable vibrational excitation without autodetachment.

To obtain the symmetry of the anion resonance state based on axial recoil approximation, we have obtained the angular distribution of OCl^- ions for KER ranging from 0.4 to 1.2 eV (Fig 2(d)). From the formalism presented by O'Malley and Taylor[33] for the diatomic case and modified by Azria *et. al*[34] for the polyatomic species, the angular distribution of the fragment ions is given by the expression

$$I(\theta) \propto \frac{1}{2\pi}\int_0^{2\pi}\left|\sum_{lm\varepsilon} i^l \exp(i\delta_l) a_{lm}^{\varepsilon}\chi_{lm}^{\varepsilon^*}(\theta,\varphi)\right|^2 d\varphi \quad (8)$$

where, $\chi_{lm}^{\varepsilon}(\theta,\varphi)$ are basis functions for the irreducible representation of the point group of the molecule, a_{lm}^{ε} their amplitude and δ_l their phase. Here, the angle θ determines the orientation of the dissociating bond with respect to the incoming electron beam. Since, OClO belongs to C_{2v} point group in equilibrium geometry and its ground state is of B_1 symmetry with an equilibrium bond angle (117.5^0), using the axial recoil approximation we have fitted the angular distribution with an incoherent sum of spherical harmonics corresponding to $B_1 \rightarrow A_1$ and $B_1 \rightarrow B_1$transitions as shown in Fig 2(d). The distribution fits with the linear combination of A_1 and B_1 states, indicating their presence in this energy range. The function used for the fit is

$$I(\theta) = I_{A_1}(\theta) + I_{B_1}(\theta) \quad (9)$$

where $I_{A_1}(\theta)$ and $I_{B_1}(\theta)$ and contributions from the $B_1 \rightarrow A_1$ and $B_1 \rightarrow B_1$transitions respectively. The corresponding fit functions used were

$$I_{A_1}(\theta) = a_1\left(1 + b_1(sin^2\theta sin^2\beta + 2cos^2\theta cos^2\beta) + {b_1}^{1/2}\, cos\delta_1 cos\beta cos\theta\right) \quad (10a)$$

$$I_{B_1}(\theta) = a_2\left(4sin^2\theta + \frac{3}{2}b_2(sin^4\theta sin^2\beta + sin^2 2\theta cos^2\beta) + 2(3b_2)^{1/2}\, cos\delta_2 cos\beta sin\theta \sin 2\theta\right) \quad (10b)$$

Here, β is the bond angle of the dissociating parent anion and we have assumed the equilibrium bond angle of the neutral OClO. For A_1 state, the contributions from *s* and *p* wave have been considered and the relative phase between these partial waves is $\delta_1$whereas for the B_1 state he contributions from *p* and *d* waves have been considered with their relative phase as δ_2. We have used these phases as well as the weight factors of these partial waves (b_1 and b_2) and the weight factors for the two distributions (a_1 and a_2) as the fitting parameters. The fit shows dominant contribution from the A_1 state compared to the B_1 state. The corresponding contribution of these states are in the ratio 5:1. In the theoretical calculation reported earlier[15] no negative ion state is reported at 0.7 eV. The resonance obtained in these calculations around 3 eV is a single particle

shape resonance of B_1 symmetry. Wei *et al*[16] have reported an anion excited state near 1.5 eV with the smaller bond angle (112^0) and similar bond length as that of neutral ground state. Our results on OCl^- validate this assignment. However, the overall dissociation process is slow in this energy range. As can be seen from the KER distributions, the smeared angular distribution may also indicate the contribution of various vibrational modes of the parent anion in the dissociation dynamics. This is also consistent with the deviation of the observed KER from that expected under the simple impact approximation.

3.2 O^- channels:

3.2.1 Peaks at 1.1 eV and 4 eV

As shown in Fig. 1, the O^- ion signal is found to peak at 1.1 eV, 4 eV, and 8 eV respectively. We have recorded momentum images around each of these peaks. The momentum image of O^- at 1.1 eV appears as a single thermal 'blob' as seen in Fig 3(a). This is consistent with the threshold of 1.09 eV for the formation of O^- + OCl ($X^2\Pi$). We were unable to determine any specific angular distribution due to low KE of the ions. The momentum image at 4 eV exhibits an outer ring with a large intensity in the forward direction and an inner 'blob' that corresponds to thermal ions as seen in Fig 3(b). From Table 1 we can see that the threshold for three-body dissociation (O^- + Cl + O) is 3.88 eV. Hence, we may attribute the inner 'blob' to this channel. As this channel may arise from two- as well as three-body dissociation of the molecule, we have plotted the KE distribution instead of the KER distribution of this ion. The KE distribution obtained from the momentum image at 4 eV is shown in Fig 3(c). Using the simple impulse approximation (Eq. 6), for the O^- + OCl ($X^2\Pi$) channel, the energy transferring into the rotational degrees of freedom is about 0.26 eV. From the KE distribution, we note that the mean KE of the outer ring is about 1.7 eV. The corresponding KER would be 2.23 eV. This together with the rotational energy of 0.26 eV and the threshold for this DEA channel of 1.09 eV implies that about 0.42 eV is transferred into the vibrational excitation of the OCl radical.

Although we have a well-defined ring for the two-body dissociation channel that peaks in the forward direction, we could not fit any angular distribution function simply because this electron capture involves a transition from B_1 state of neutral and this state does not support any angular distribution that peaks in the 0^o and 180^o. Marston *et al.*[14] attributed this peak to the core-excited

resonance. Baluja *et al.*[15] obtained single particle shape resonances (of B_1 symmetry) around 2.96 eV and 5.75 eV. As we could not determine the symmetry of the anion state at this energy, we believe that this channel may involve substantial rearrangement before dissociation.

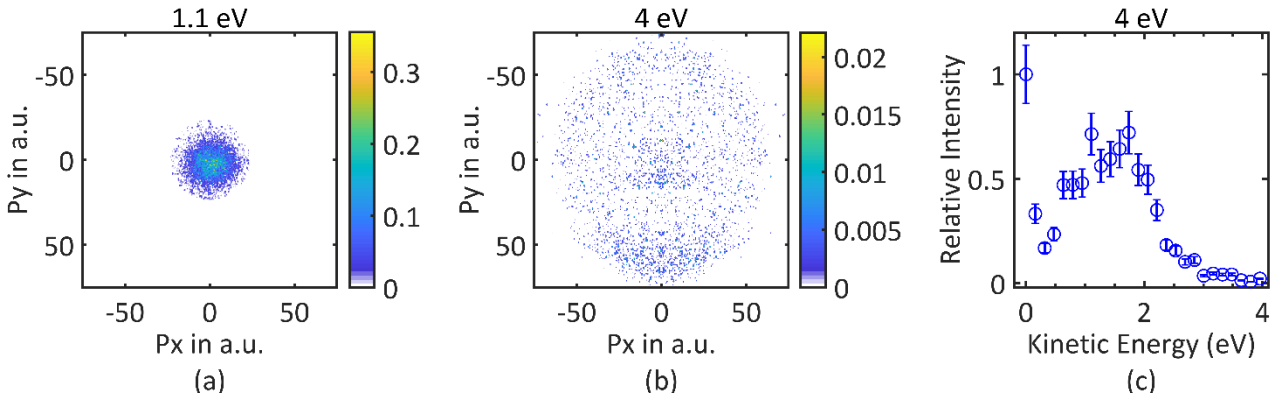

Fig. 3 Momentum image of O^- at (a) 1.1 eV and (b) 4 eV with the direction of the electron beam from top to bottom and (c) the kinetic energy distribution at 4 eV.

3.2.2 O^- Channel: 8 eV peak

The momentum image of O^- obtained at 8 eV exhibits a distinct ring as seen in Fig 4(a) and the corresponding KE distribution is shown in Fig 4(b). The KE distribution peaks at 2 eV which corresponds to a KER of 2.62 eV. There are two channels that can possibly contribute to this ring. First is the two-body dissociation of $OClO^-$ to O^- + OCl ($A^2\Pi$) (threshold 5.01 eV). The other channel being that of three-body dissociation. The lower energy O^- + OCl ($X^2\Pi$) channel will leave the OCl with enough internal energy to undergo further breakup leading to three-body dissociation. In the OCl ($A^2\Pi$) channel, the excess energy available in the system is about 2.99 eV out of which about 0.27 eV will be in rotational excitation according to the simple impulse approximation (Eq. 6). This and the KER of 2.62 eV accounts for 2.89 eV of the excess energy. Hence, the remaining 0.1 eV ought to go into vibrational excitation of the OCl fragment.

For the case of three-body fragmentation, the KE distribution that will depend on the geometry of the parent anion at the time of dissociation. If this fragmentation initiates with the bending of $OClO^-$ along with a symmetric stretch, both the bonds would dissociate and all three atoms would fly away from each other. In such a case, the KE ratios of the fragments depend on the bond angle at the time of dissociation. By knowing the total energy available for KER and measuring the

kinetic energy of any fragment, one can obtain the bond angle before concerted dissociation. Assuming concerted three-body dissociation channel and applying linear momentum conservation, we obtain a bond angle of about 160^o (±10 ^{o}) for the O^- ions with KE of 2 eV. The angular distribution obtained for this channel shown in Fig 4(c) peaks at about 105^o. The angular distribution of Cl^- formed at this resonance peaks at 0^o and 180^o (Fig. 7, see below). Based on this, we conclude that this Cl^- channel is most active when the anion resonance is formed with the electron beam approaching the molecule along its principal axis. By assuming this orientation of the molecule with the electron beam direction and using the information that the O^- angular distribution peaks at 105^o we obtain the bond angle at the time of dissociation to be 150^o (2 x (180-105)^o) which is consistent with our estimate of 160^o based on the observed KE. At 8 eV, Baluja *et al.*[15] obtained a single particle shape resonance of A_2 symmetry however, the dynamics we observe is not consistent with this symmetry.

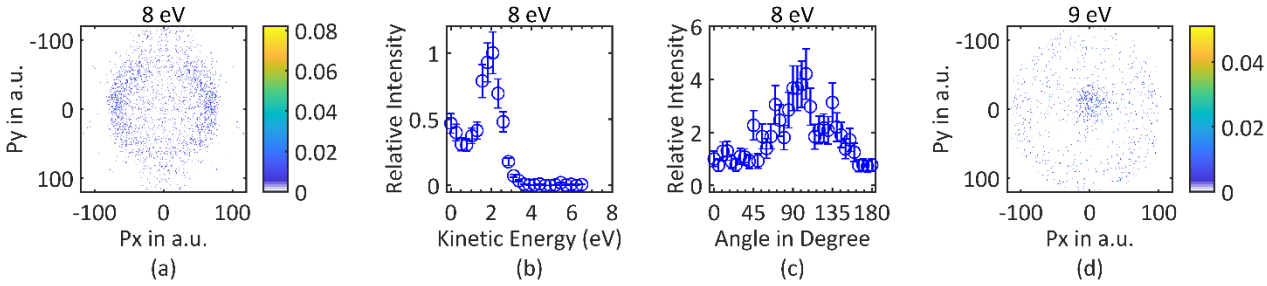

Fig. 4 (a) Momentum image of O^- at 8 eV (electron beam direction from top to bottom) and corresponding (b) kinetic energy distribution (c) angular distribution and (d) momentum image at 9 eV.

As we increase the electron energy to 9 eV, we observe that an isotropic thermal 'blob' starts to appear along with the earlier observed outer ring, as seen in Fig 4(d). We know that the energy required for three-body dissociation (O^- + Cl (^3P) + O (^3P)) is 3.88 eV and the energy required for O (^1S) is 4.19 eV. Thus, the energy required for three-body dissociation (O^- + Cl (^3P) + O (^1S)) is about 8 eV. The production of thermal O^- ions may also be explained as due to a sequential dissociation in which an O atom in ^1S state leaves first with most of the excess energy and the remaining molecular anion dissociates further producing O^- and Cl atom.

3.3 Cl^- & O_2^- Channels:

The signal corresponding to ions of mass 32 - 35 peaks around 0.7 eV, 4 eV, and 8 eV. We cannot distinguish between the contribution from O_2^- and Cl^- due to our poor mass resolution. However, from the literature, we know that O_2^- contributes only to the 0.7 eV peak[13,14]. Below we analyze the momentum images obtained around each of these peaks.

3.3.1 Peak at 0.7 eV

The momentum image obtained at 0.7 eV is shown in Fig 5(a). As we cannot distinguish between the two ions that contribute at this energy, we have plotted KE distribution instead of KER for this peak in Fig 5(b) as KER for both the channels will be different for a given KE of the fragment. Both the Cl^- channel and the O_2^- channel arise from the symmetric dissociation of the resonant state. Since the three-body dissociation threshold for the formation of Cl^- is 1.73 eV (Table 1), its formation at this resonance is energetically possible only if the neutral fragment is O_2. The O_2 thus formed is likely to be in high vibrational states.

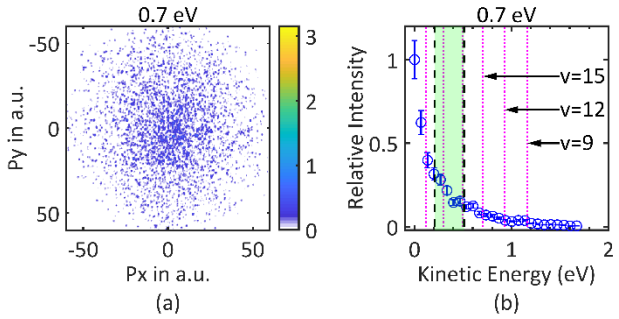

Fig. 5 (a) Momentum image of Cl^- (and O_2^-) at 0.7 eV (electron beam direction from top to bottom) and (b) the kinetic energy plot of the corresponding image. The vertical solid magenta lines indicate the kinetic energy of Cl^- where the O_2 is produced in electronic ground state with vibrational excitation (v). The vertical dotted black lines indicate the limits of kinetic energy of O_2^- ions as explained in the text.

As the KE spectrum shows substantial spread, it indicates internal excitation of the molecular fragment. In the O_2^- channel the maximum KE would be 0.51 eV as the threshold for this channel is -0.27 eV. However, the internal excitation of the observed O_2^- ion cannot exceed 0.57 eV, which is its autodetachment threshold[35]. Thus the minimum KE would be 0.21 eV and consequently, the O_2^- contribution in the observed KE spectrum will only be between 0.21 eV and 0.51 eV, as shown by green shaded region in Fig 5(b). On the other hand, the Cl^- channel (threshold -3.43 eV) could contribute across the entire KE range and the corresponding O_2 fragment will be left with a high

degree of vibrational excitation. This is shown by vertical magenta lines in Fig 5(b). As can be seen from the figure, the Cl^- production with O_2 in the electronic ground state favours high vibrational excitation (from v=11 to v=26). However, for such a high vibrational excitation the bond length of O_2 should be much higher than its equilibrium bond length. In the equilibrium geometry of OClO, the O-O distance is about 2.51 Å[36] and the outer turning point of the v=26 level in O_2 is about 1.85 Å[37]. This indicates the important role of the bending motion of parent anion before or during dissociation. However, we cannot rule out the two other channels leading to Cl^- formation with O_2 being formed in electronic excited states, namely $Cl^- + O_2$ ($^1\Delta_g$) (threshold: -2.45 eV) and $Cl^- + O_2$ ($b^1\Sigma^+_g$) (threshold: -1.79 eV). In both of these cases the minimum excess energy that will result in the vibrational excitation would be about 1.04 eV and 0.38 eV (corresponding to 1 eV in KE of Cl^-). This implies that for these channels the vibrational excitation would range in v=5 to 20 and v=2 to 16 respectively. Hence, even these channels would also involve substantial bending mode excitation of the parent anion.

The theoretical calculations by Baluja *et al.*[15] found no anion state in this energy range whereas Wei *et al.*[16] reported a pair of B_1 states in the energy range of 1 to 2 eV with an equilibrium bond length close to that of the neutral ground state. However, in this state they have found the equilibrium bond angle to be smaller indicating effective bending excitations from the Frank-Condon transition. The configuration of this state is also found to be a doubly occupied $3b_1$ orbital which is known to be bonding along the terminal O atoms and antibonding about the O-Cl bond. The description of this state fits well with the observed dissociation dynamics.

3.3.2 Peak at 4 eV

The momentum image at 4 eV is shown in Fig 6(a). As can be seen from the figure and the extracted KE distribution (Fig 6(b)), the maximum KE observed is about 0.45 eV. With this KE of the ion, the internal excitation energy of the fragments would be at least 3 eV. The first two excited states of Cl atom are at energy 0.11 eV and 8.9 eV respectively from which the second state is energetically not accessible. This implies that if the signal corresponds to the O_2^- channel, this ion would accommodate about 3 eV as internal energy. As argued earlier, with so much excess energy, this ion would not survive the autodetachment and it cannot be detected in mass spectrometer. Hence, we conclude that in this peak the sole contributor is the Cl^- species. This is

consistent with the previous reports[13,14] that only Cl^- ion is formed at this energy. Marston *et al.*[14] reported the Cl^- ion energy is thermal. The present KE distribution, as well as the momentum image, shows some structure around 0.24 eV. Based on the energy threshold (-3.43 eV, -2.45 eV and -1.79 eV) for Cl^- channel with O_2 in the ground state ($X^3\Sigma_g^-$) or first two electronic excited states ($a^1\Delta_g$, $b^1\Sigma_g^+$), the available excess energy in the system is about 7.43 eV, 6.45 eV and 5.79 eV respectively. The bond dissociation energy of O_2 in the ground state is 5.1 eV. This implies that any two-body dissociation channel with O_2 in any one of the energetically accessible electronic state with the dissociation limit O (^3P) + O (^3P) will not give this KE distribution. Hence, we conclude that the Cl^- observed around this peak is most likely to arise from a three-body break-up. The threshold for this process is 1.73 eV. As discussed earlier, there are two possibilities of three-body dissociation namely a sequential or a concerted channel. Considering the dissociation takes place immediately from the equilibrium geometry of the molecule at the time of electron capture, the maximum KE of Cl^- is expected to be about 0.44 eV. The observed KE distribution implies that such dissociation necessarily starts with the bond angle in the parent anion larger than the one in the equilibrium geometry. On the other hand, concerted dissociation with one of the O atom in ^1D excited would correspond to maximum KE in the Cl^- channel of about 0.07 eV whereas in the case of sequential three-body dissociation, the lower values of KE indicate that the first O atom takes away a substantial amount of excess energy as its KE. Here again, the first dissociating O atoms can also be in the excited state. In the KE distribution that we have obtained, it is difficult to pin-point any of the above channels. However, in the Cl^- kinetic energy range of 0.07 eV to 0.44 eV, we may conclude that the sequential dissociation and the concerted dissociation with one of the O atoms in the ^1D state do not contribute and it is solely a concerted dissociation with both O atoms in the ^3P state.

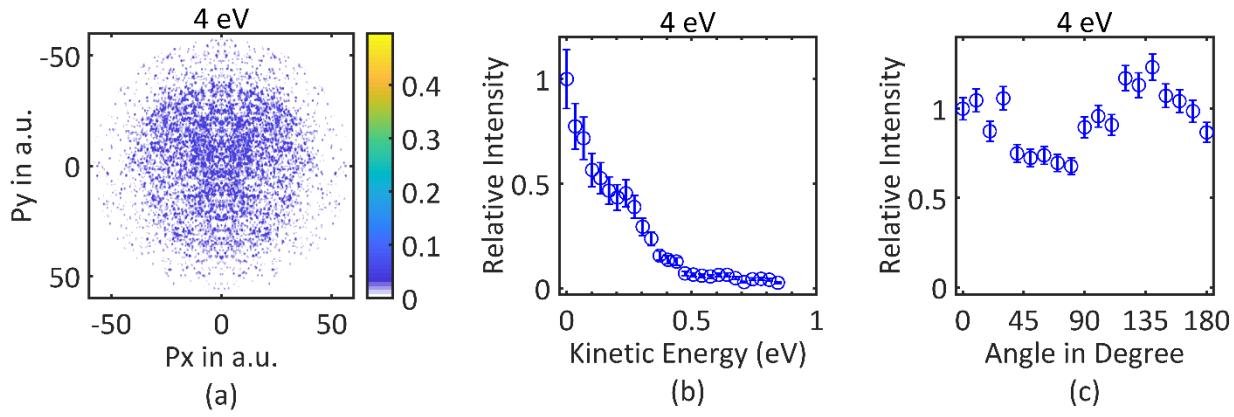

Fig. 6 (a) Momentum image of Cl^- at 4 eV (electron beam direction from top to bottom) and (b) kinetic energy distribution of the same image and (c) Angular distribution for ions with KE in the range 0.07 eV - 0.44 eV.

The angular distribution of the ions in the above kinetic energy range is shown in Fig 6(c). The distribution exhibits forward-backward asymmetry with more intensity in the backward direction and peaking at 130^o ($\pm 10^0$). Such an anisotropic distribution is most likely to arise from the concerted dissociation. The KE in this range corresponds to the dissociation with both the O atoms in their ground state (^{3}P). One possibility of getting such a distribution in concerted dissociation under the axial recoil approximation would be if the incoming electron approaches along one of the O-Cl bonds. In this case, the principal axis of the molecule would be at 122^o which will also be the direction of the Cl^-. In other orientation, the Cl^- ion will be ejected along 58^o. As discussed in the earlier report by Marston *et al.*[14], this channel is likely to arise from a core-excited resonance.

3.3.3 Peak at 8 eV

Momentum images obtained around 8 eV electron energy, exhibit a distinct ring as shown in Fig 7. With increase in electron energy the ring size increases without any change in angular distribution. The mean KE of the ring obtained by us at 8 eV electron energy is 0.25 eV. As argued earlier, based on this KE measurement, we conclude that the signal at this electron energy entirely arises from the Cl^- ions. Marston *et al.*[14] have reported the KE of Cl^- to be 0.5 eV at 8 eV electron energy. Momentum analysis for the concerted three-body fragmentation confirms that if Cl^- is produced with 0.25 eV along with both the O atoms in ^3P state, the bond angle of $OClO^-$ at the time of dissociation would be close to 155^o. The oxygen atoms, in this case, will have a KE of

about 3 eV each. However, there are other possibilities like O atoms being formed in an excited state (^1D) which can also lead to low energy Cl^- ion. In this case, the bond angle of parent anion ($OClO^-$) at the time of dissociation would be 150°. The momentum image of these ions shows an angular distribution with lobes in the forward and backward directions with more intensity in the forward direction (Fig 7(d)). Moreover, this angular feature does not change with the change in incoming electron energy as seen in Fig 7. Therefore, under the axial recoil approximation, we conclude that the electron capture takes place along the principal axis and at the time of dissociation Cl atom is oriented opposite to the direction of momentum vector of the incoming electron. This is possible as at this energy the core-excited resonances are expected to play a role which can involve a_1 orbital that can interact with electron along the principal axis. The theoretically obtained[12] single particle shape resonance of B_1 symmetry cannot explain these dynamics.

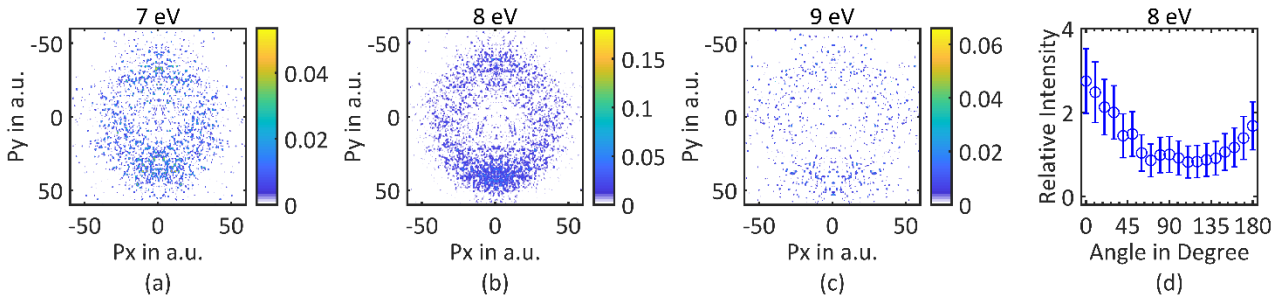

Fig. 7 Momentum image of Cl^- at (a) 7 eV, (b) 8 eV and (c) 9 eV (electron beam direction from top to bottom) and (d) angular distribution of Cl^- obtained at 8 eV electron energy.

The consistent picture emerging from the angular distribution and KE distribution of Cl^- and O^- ion at 8 eV indicates that both the ions result from a three-body fragmentation of the same negative ion resonance state of $OClO^-$ starting from same geometry. The cross section for each channel indicates the branching ratio as well as the survival probability along that channel. From our analysis of the kinetic energy and angular distributions of O^- and Cl^-, we conclude that at 8 eV, $OClO^-$ is undergoing concerted three-body dissociation with the bond angle about 150° at the time of dissociation. Since the angular distribution for Cl^- is peaking at 0° and 180°, the probability of this channel appears to be maximum when the incoming electron approaches along the principal axis of the molecule. Moreover, from the forward backward asymmetry observed in the Cl^-

channel and peak in the O^- signal around 105°, we infer that these channels are more active when the parent anion is formed with the capture of electron from the O side of the molecule.

3.4 Consequences for Stratospheric Chemistry; Further Reaction with Ozone:

The major channel (about 90%) is OCl^- + O. Thus the ability of this ion to react further with ozone will dominate the ozone destruction mechanism. This will depend hugely on the internal energy of OCl^- produced. The possible reactions of OCl^- and Cl^- with ozone and their threshold energies is given in Table 2. The thermodynamic thresholds are calculated using $\Delta H_{0f}(OCl)$ = 1.05 eV, $\Delta H_{0f}(O)$ = 2.58 eV, $\Delta H_{0f}(Cl)$ = 1.26 eV, $\Delta H_{0f}(O_3)$ = 1.48 eV[23], $\Delta H_{0f}(ClO_2)$ = 1.07 eV[38], $\Delta H_{0f}(OClO)$ = 1.08 eV, $\Delta H_{0f}(ClO_3)$ = 1.99 eV[39], EA(OCl) = 2.28 eV, EA(ClO_2) = 2.37 eV[40] and EA(ClO_3) = 4.25 eV[41].

From our kinetic energy release measurements employing VSI technique, we see that maximum internal energy of OCl^- produced via DEA is about 1.2 eV and the maximum kinetic energy observed for OCl^- ion is also about 0.3 eV. Thus, the reaction of OCl^- with ozone leading to the production of active Cl (threshold 0.56 eV) for the catalytic cycle may not be effective from the vibrationally ground state anion. However, vibrationally excited slow OCl^- may become an important species in this reaction, especially in view of the large cross section for its formation[9].

From Table 2 we can see that the reactions 2 and 7 involving OCl^- and Cl^- have negative thresholds and they lead to formation of Cl^- and OCl^- respectively while converting O_3 to O_2. Thus, these channels with anions as products can continue cyclically and keep destroying ozone, provided they are not destroyed by other processes including photodetachment. However, upon photodetachment, these anions will be converted into their neutral forms, which may still play a role in catalytic cycle that destroys ozone. In addition, these anions may produce other neutral radicals important for the catalytic cycle involved in the destruction of ozone. Thus, in order to understand the role of DEA to OClO in ozone destruction, it is important to study the role of these radical anions and their life cycle in the upper atmosphere.

In O^- channel at 4 eV, the OCl radical is produced with almost 0.4 eV internal energy and at 8 eV it is produced with electronic excitation to $A^2\Pi$ state. Although the cross section for this channel is small, such vibrationally or electronically excited species produced in the cold upper atmosphere

may have more significance in the catalytic cycle. In all the DEA channels, Cl is produced with KE up to 0.5 eV, which may also be important in the catalytic cycle.

Table 2 Possible reactions of OCl^- and Cl^- with ozone along with their threshold energies.

	Dissociation Channel	Threshold (eV)
1	$OCl^- + O_3 \rightarrow O_2^- + O_2\left(X^3\Sigma_g^-\right) + Cl(X^2P)$	0.56
2	$OCl^- + O_3 \rightarrow Cl^- + 2O_2\left(X^3\Sigma_g^-\right)$	-2.60
3	$OCl^- + O_3 \rightarrow ClO_2^- + O_2\left(X^3\Sigma_g^-\right)$	-1.55
4	$OCl^- + O_3 \rightarrow ClO_3^- + O\ (^3P)$	0.07
5	$Cl^- + O_3 \rightarrow O_2^- + OCl\ (X^2\Pi)$	1.47
6	$Cl^- + O_3 \rightarrow O^- + OClO$	3.07
7	$Cl^- + O_3 \rightarrow OCl^- + O_2\left(X^3\Sigma_g^-\right)$	-0.36

4 Conclusions

We have unraveled the details of the dynamics behind DEA to the atmospherically important OClO molecule. DEA to OClO leads to the production of OCl^-, Cl^-, O_2^- and O^-. The OCl^- yield peaks around 0.7 eV and around this peak, the OCl^- is produced with O atoms only in the (^3P) state but as the electron energy increases, the excess energy appears in the vibrational excitation of the anion. We attribute this channel to the resonant states with A_1 and B_1 symmetry, contributing in the ratio 5:1. At 0.7 eV both Cl^- and O_2^- are produced via symmetric dissociation with relatively faster dissociation resulting in the production of Cl^-. At 4 eV Cl^- is produced via concerted three-body dissociation following the electron capture. In this case, the concerted dissociation appears to result from the electron capture with its momentum vector along one of the O-Cl bonds. The O^- yield peaks at 1.1 eV, 4 eV and 8 eV. At 1.1 eV, O^- is produced with OCl ($X^2\Pi$). At 4 eV, O^- is produced via two different processes - three-body dissociation (O^- + Cl + O) with low KER and two-body dissociation (O^- + OCl ($X^2\Pi$)) with distinctly higher KER and some 0.4 eV going into the vibrational excitation of OCl. However, we could not assign a specific anion state to this channel. At 8 eV both Cl^- and O^- are produced from the same NIRS through concerted three-body dissociation. The momentum distributions of the ions indicate that the electron approaching along

the principal axis of the molecules has maximum probability for capture and that the NIRS will have a bond angle of 150^o – 160^o at the time of dissociation.

All of the various fragment anions produced in DEA process have sufficient internal energy as well as kinetic energy to be relevant for the ozone destructing catalytic cycle. However, the role of Cl^- and OCl^- needs to be studied more carefully in order to understand the importance of DEA to OClO in ozone destruction mechanism. With such rich dynamics observed in such an important molecule, our results highlight the dire need for complementary theoretical calculations to fully understand the DEA process and its role in the chemistry of the upper atmosphere.

Acknowledgement

We would like to express our appreciation for the scientific contributions of Prof. Mike Ashfold, both as a friend and a collaborator, and for whom this issue is dedicated on his 65^{th} birthday.

References

[1] M. J. Molina and F. S. Rowland, *Nature*, 1974, **249**, 810–812.

[2] V. Vaida and J. D. Simon, *Science*, 1995, **268**, 1443–1448.

[3] Michael B. McElroy, Ross J. Salawitch, Steven C. Wofsy and Jennifer A. Logan, *Nature*, 1986, **321**, 759.

[4] L. T. Molina and M. J. Molina, *J. Phys. Chem.*, 1987, **91**, 433.

[5] Susan Solomon, Rolando R. Garcia, F. Sherwood Rowland and Donald J. Wuebbles, *Nature*, 1989, **321**, 755.

[6] Stanley P. Sander, Randall R. Friedl and Yuk L. Yung, *Science*, 1989, **245**, 1095.

[7] R. F. Delmdahl, D. H. Parker and A. T. J. B. Eppink, *J. Chem. Phys.*, 2001, **114**, 8339.

[8] H. F. Davis and Y. T. Lee, *J Chem Phys*, 1996, **105**, 8142–8163.

[9] V. Vaida, S. Solomon, E. C. Richard, E. Ruhl and A. Jefferson, *Nature*, 1989, **342**, 405–408.

[10] J. L. Gole, *J Phys Chem*, 1980, **84**, 1333–1340.

[11] W. G. Lawrence, K. C. Clemitshaw and V. A. Apkarian, *J. Geo. Res. Atomsphere*, 1990, **95**, 18591.

[12] M. Meinke, C. Schmale, E. Ruhl and E. Illenberger, *17th Int. Conf. on Physics of Electronic and Atomic Collisions (Brisbane) Abstracts*, 1991, 262.

[13] G. Senn, H. Drexel, G. Marston, N. J. Mason, T. D. Mark, M. Meinke, C. Schmale, P. Tegeder, E. Ruhl and E. Illenberger, *J Phys B: At Mol and Opt Phys*, 1999, **32**, 3615.

[14] G. Marston, I. C. Walker, N. J. Mason, J. M. Gingell, H. Zhao, K. L. Brown, F. Motte-Tollet, J. Delwiche and M. R. F. Siggel, *J Phys B: At Mol and Opt Phys*, 1998, **31**, 3387.

[15] K. L. Baluja, N. J. Mason, L. A. Morgan and J. Tennyson, *J Phys B: At, Mol and Opt Phys*, 2001, **34**, 4041.

[16] Z. Wei, B. Li, H. Zhang, C. Sun and K. Han, *J. Comput. Chem.*, 2007, **28**, 467.

[17] D. Nandi, V. S. Prabhudesai, E. Krishnakumar and A. Chatterjee, *Rev. Sci. Instrum.*, 2005 **76**, 053107.

[18] E. Krishnakumar, S. Denifl, I. Cˇadezˇ, S. Markelj and N. J. Mason, *Phys. Rev. Lett*., 2011 **106**, 243201.

[19] K. Gope, V. S. Prabhudesai, N. J. Mason and E. Krishnakumar, *J. Phys. B: At. Mol. Opt. Phys.*, 2016 **49**, 015201.

[20] E. Szymanska, V. S. Prabhudesai, N. J. Mason and E. Krishnakumar, *Phys Chem Chem Phys*, 2013, **15**, 998–1005.

[21] K. Gope, V. Tadsare, V. S. Prabhudesai, N. J. Mason and E. Krishnakumar, *Euro Phys J D*, 2016, **70**, 134.

[22] R. I. Derby, W. S. Hutchinson, T. H. Dexter and J. M. Naughton, *Chlorine (IV) Oxide*, John Wiley and Sons, Inc., 2007, pp. 152–158.

[23] M. W. Chase Jr, *J. Phys. Chem. Ref. Data, Monograph*, 1998, **9**, 1.

[24] J. D. Cox, D. D. Wagman and V. A. Medvedev, *CODATA Key Values for Thermodynamics*, Hemisphere Publishing Corp., New York, 1984, 1

[25] V. Distelrath and U. Boesl, *Faraday Disc. Chem. Soc.*, 2000, **115**, 161.

[26] K. M. Ervin, W. Anusiewicz, P. Skurski, J. Simons, and W. C. Lineberger, *J. Phys. Chem. A*, 2003, **107**, 8521

[27] C. Blondel W. Chaibi, C. Delsart, C. Drag,, F. Goldfarb, S. Kröger, *E. Phys. J. D*, 2005, **33**, 335

[28] R. Trainham, G. D. Fletcher, and D. J. Larson, *J. Phys. B: At. Mol. Opt. Phys.*, 1987, **20**, L777

[29] K. P. Huber and G. Herzberg, *Molecular Spectra and Molecular Structure IV – Constants of Diatomic Molecules*, Van Nostrand Reinhold Company, New York, 1979.

[30] A. Kramida, Yu. Ralchenko, J. Reader and NIST ASD Team, *NIST Atomic Spectra Database ver. 5.6.1*, https://physics.nist.gov/asd 2018

[31] K. Gope, V. S. Prabhudesai, N. J. Mason and E. Krishnakumar, *J Chem Phys*, 2017, **147**, 054304.

[32] K. Gope, V. Tadsare, V. S. Prabhudesai and E. Krishnakumar, *Euro Phys J D*, 2017, **71**, 323.

[33] T. F. O'Malley and H. S. Taylor, *Phys Rev*, 1968, **176**, 207–221.

[34] R. Azria, Y. L. Coat, G. Lefevre and D. Simon, *J Phys B: At Mol Phys*, 1979, **12**, 679.

[35] Dake Yu, David A. Armstrong and Arvi Rauk, *J. Chem. Phys.*, 1992, **97**, 5522.

[36] K. Miyazaki, M. Tanoura, K. Tanaka and T. Tanaka, *J. Mol. Spect.*, 1986, **116**, 435

[37] F. R. Gilmore, *J. Quant. Spectrosc. Radiat. Transfer*, 1965, **5**, 369.

[38] J. S. Francisco and S. P. Sander *The Journal of Chemical Physics*, 1993, **99**, 2897

[39] Matthew M. Mayer and Steven R. Kass, *J. Phys. Chem. A*, 2010, **114**, 4086.

[40] L. M. Babcock, T. Pentecost and W. H. Koppenol, *J. Phys. Chem.*, 1989, **93**, 8126.

[41] S. B. Wang and L. S. Wang, *J. Chem. Phys.*, 2000, **113**, 10928.